

## Supporting Information for

# Heterogeneous OH oxidation of primary brown carbon aerosol: effects of relative humidity and volatility

*Elijah G. Schnitzler,\*† Tengyu Liu, Rachel F. Hems, Jonathan P. D. Abbatt*

Department of Chemistry, University of Toronto, Toronto, ON M5S 3H6, Canada

### Corresponding Author

\*E-mail: elijah.schnitzler@okstate.edu.

### Present Address

†Department of Chemistry, Oklahoma State University, Stillwater, OK 74078

## Contents

<b>Fig. S1</b> Times series of absorption coefficient and absorption coefficient divided by the geometric cross section during experiments at 60 % RH.	S3
<b>Fig. S2</b> Times series of relative geometric mean surface diameter and relative absorption during two particle-loss control experiments at 15 % RH.	S4
<b>Fig. S3</b> Time series of relative absorption during photolysis control experiments.	S5
<b>Fig. S4</b> Times series of relative geometric mean surface diameter during heterogeneous OH oxidation experiments at 60 % RH and 15 % RH.	S6
<b>Fig. S5</b> Times series of absorption coefficient at 405 nm, geometric cross section, and relative absorption.	S7
<b>Fig. S6</b> Representative mass spectra of the organic fraction in terms of absolute contributions of fragments to the total and differences between spectra before and after 3 hr of OH exposure.	S8
<b>Fig. S7</b> Representative times series of the contribution of $m/z$ 44 and 60 to the total organic signal ( $f_{44}$ and $f_{60}$ , respectively) during heterogeneous OH oxidation.	S9

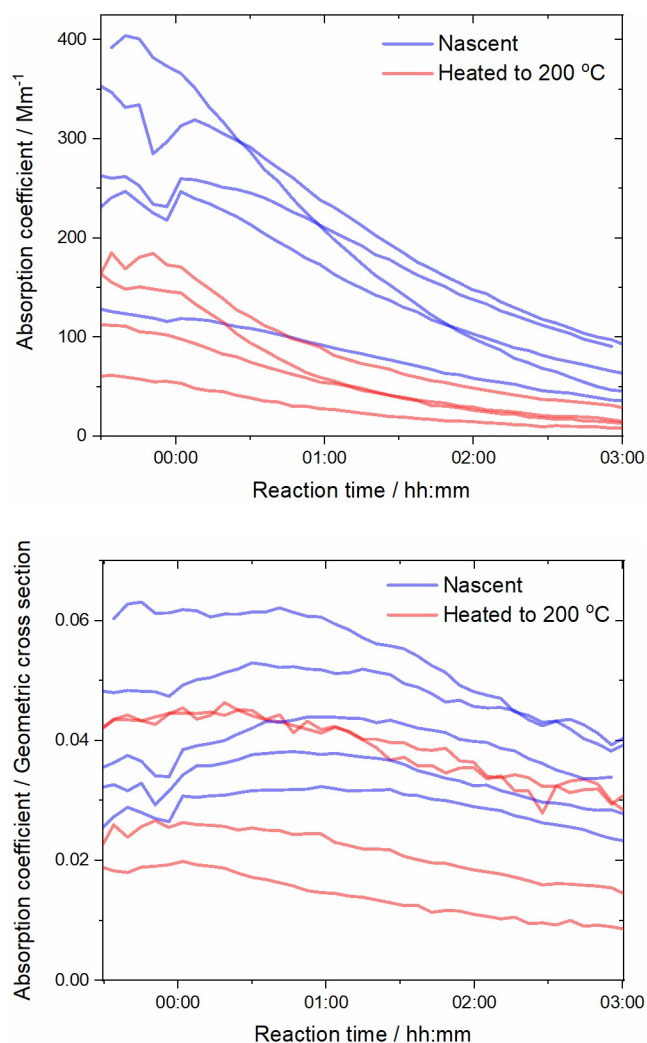


**Fig. S1** Times series of (top) absorption coefficient at 405 nm, measured using the photoacoustic spectrometer, and (bottom) absorption coefficient divided by the geometric cross section per unit volume, measured by the scanning mobility particle spectrometer, during all replicate experiments at 60 % RH. The average of the initial normalized absorption values, shown in the bottom panel, was lower for the four heated particle samples than the five nascent particle samples, but the values are overlapping when the large standard deviations between replicates:  $0.03 \pm 0.01$  and  $0.04 \pm 0.01$ , respectively. Similarly, for the experiments at 15 % RH, not shown, the values for heated and nascent particles are overlapping:  $0.04 \pm 0.01$  and  $0.05 \pm 0.02$ , respectively.

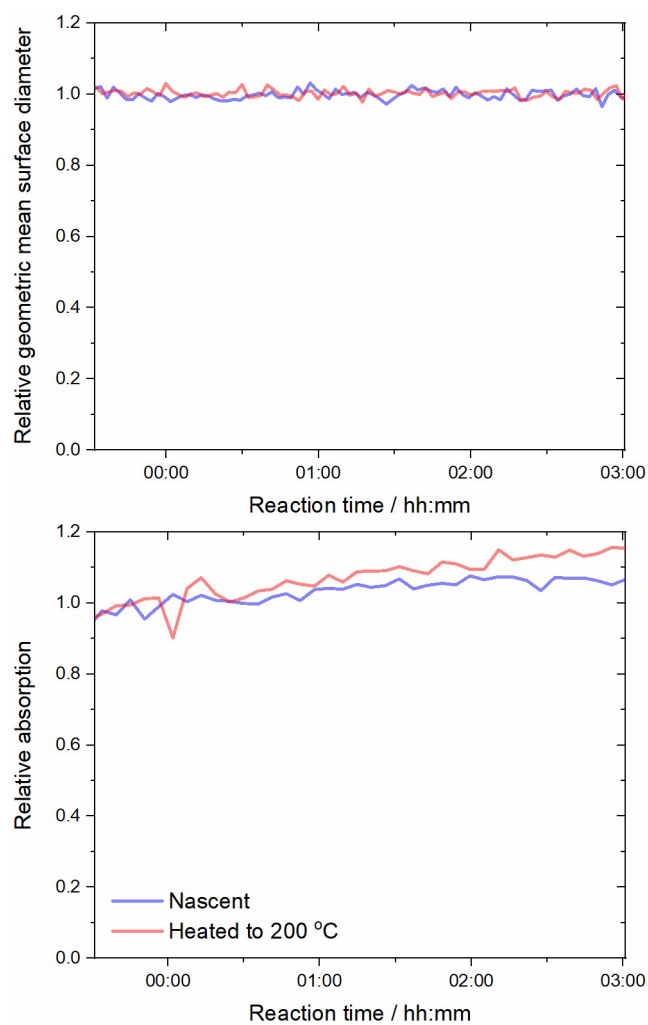


**Fig. S2** Times series of (top) relative geometric mean surface diameter and (bottom) relative absorption at 405 nm during two particle-loss control experiments at 15 % RH.

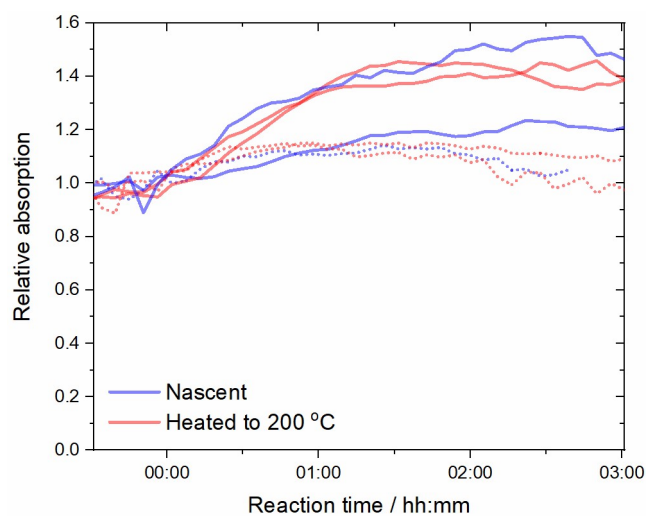


**Fig. S3** Time series of relative absorption at 405 nm during photolysis control experiments. The solid and dotted curves denote 60 and 15 % RH, respectively.

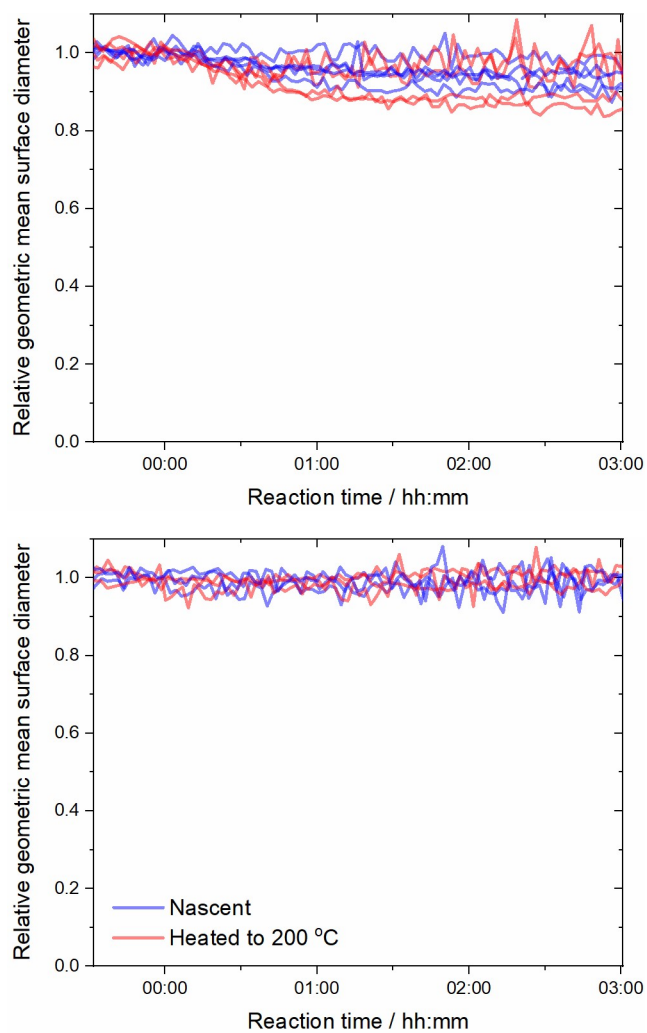


**Fig. S4** Times series of relative geometric mean surface diameter during heterogeneous OH oxidation experiments at (top) 60 % RH and (bottom) 15 % RH.

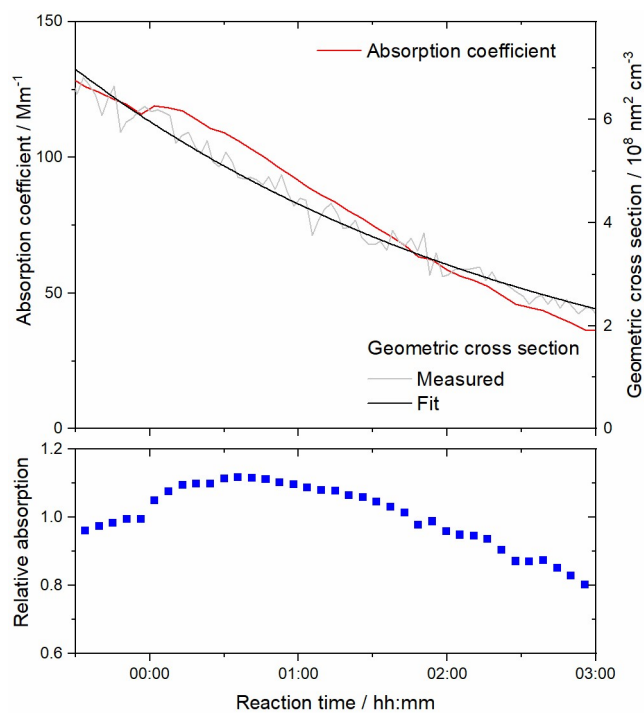


**Fig. S5** Times series of (top) absorption coefficient at 405 nm and geometric cross section and (bottom) relative absorption at 405 nm, taken as  $[\text{absorption\_coefficient}(t)/\text{cross\_section}(t)]/[\text{absorption\_coefficient}(0)/\text{cross\_section}(0)]$  of nascent particles during a typical photo-oxidation experiment at 60 % RH.

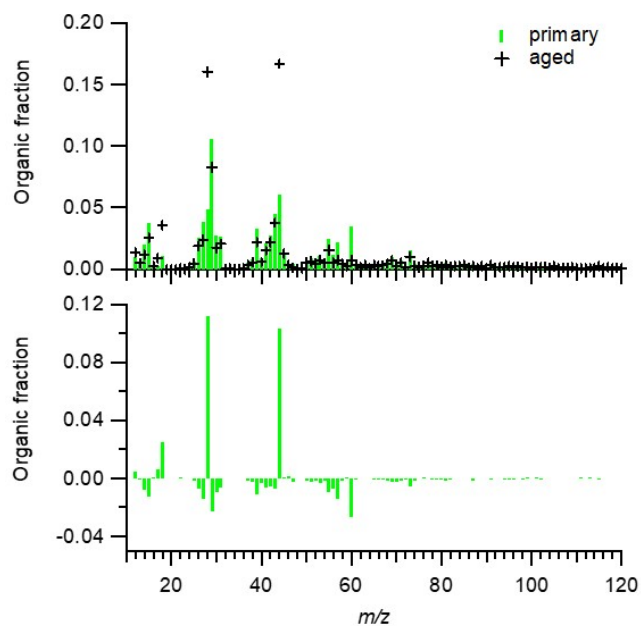


**Fig. S6** Representative mass spectra of the organic fraction in terms of (top) absolute contributions of fragments to the total and (bottom) differences between spectra before and after 3 hr of OH exposure, from which the significant increase in  $m/z$  44 and decrease in  $m/z$  60 are evident. The aerosol was heated to 200 °C, and the chamber was conditioned to 15 % RH.



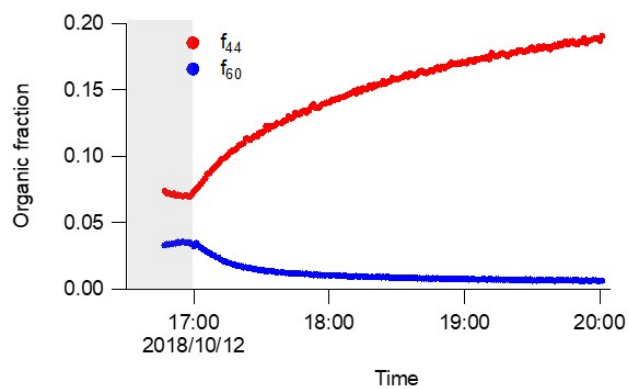


**Fig. S7** Representative times series of the contribution of  $m/z$  44 and 60 to the total organic signal ( $f_{44}$  and  $f_{60}$ , respectively) during heterogeneous OH oxidation. The grey bar denotes the period before the chamber was irradiated. The aerosol was heated to 200 °C, and the chamber was conditioned to 15 % RH.